



An ADCP-Based Data-Driven Framework for Proxy Sediment Transport Monitoring: From Controlled Flumes to Natural Rivers

Mohammd Tanvir Haque Tuhin^{1,2}, Reinhard Hinkelmann², Christoph Mudersbach¹

5 ¹Institute of Hydraulic Engineering and Hydromechanics, Department of Civil and Environmental Engineering, Bochum University of Applied Sciences, Bochum, 44801, Germany

²Chair of Water Resources Management and Modeling of Hydrosystems, Institute of Civil Engineering, Technische Universität Berlin, Berlin, 13355, Germany

Correspondence to: Mohammd Tanvir Haque Tuhin (mohammd.tuhin@hs-bochum.de)

10 Abstract.

Acoustic Doppler Current Profilers (ADCPs) provide a rich yet underutilized source for monitoring hydrodynamics and sediment transport. Accurate prediction of sediment-related variables is critical for river engineering, morphological studies, and environmental management. Among these, Bottom-Track Velocity (BT_Vel) serves as a robust proxy for near-bed sediment dynamics and bedload activity. This study develops a machine learning (ML) and deep learning (DL) framework to predict BT_Vel from ADCP-derived hydrodynamic and acoustic features, enabling proxy estimation of sediment transport processes in both controlled flume and natural riverine environments. Two datasets were analyzed: (i) a laboratory dataset of 22,650 ensemble samples obtained under controlled flow regimes, and (ii) a field dataset of 5,900 ensemble samples collected across seven campaigns at a fixed river cross-section. A consistent benchmarking strategy was applied across Random Forest, Gradient Boosting, LightGBM, CatBoost, XGBoost, LSTM, GRU, CNN, RNN, ANN, and a hybrid LSTM+CNN, with evaluation based on both an 80/20 split and a stratified 5-fold cross-validation (CV). SHAP analysis was conducted for model interpretability. In the laboratory, Random Forest ($R^2 = 0.804$ split / 0.783 CV) and Gradient Boosting (0.787 / 0.757) achieved the best generalization, while LSTM+CNN (0.770 / 0.730) and LSTM (0.775 / 0.718) remained competitive. In the field, Random Forest again delivered the strongest results (0.573 / 0.603), followed closely by CatBoost, LightGBM, and XGBoost. Notably, LSTM improved under cross-validation (0.468 \rightarrow 0.529), suggesting fold-wise diversity stabilized training under noisy, heterogeneous river data. By contrast, the Stacking Regressor consistently showed the weakest generalization across both environments. SHAP revealed a shift in feature relevance: in the laboratory, Mean water velocity (Mean_Speed) dominated predictions, while in the field, Depth and signal-to-noise ratio (SNR) emerged as stronger drivers, reflecting the influence of stage variability and acoustic quality. Overall, the study demonstrates that ADCP-derived features, coupled with explainable ML/DL models, provide robust potential for proxy sediment transport modeling. Conversion to absolute transport rates requires paired sediment measurements, while future work should expand field campaigns and explore hybrid physics–data frameworks toward operational forecasting.



1 Introduction and Objectives

Hydrodynamics and sediment transport processes are fundamental to the evolution, stability, and management of riverine and coastal environments. These intertwined processes control channel morphology, influence flood risk, affect infrastructure, and sustain aquatic ecosystems (Garcia, 2008; Frings and Vollmer, 2017; Latosinski et al., 2017). Accurate monitoring of bedload and suspended sediment flux is notoriously challenging due to the need for in-situ sampling during dynamic flow events. Traditional methods, such as physical bedload samplers (e.g. Helley-Smith traps) or sediment traps are labor-intensive, costly, and often yield sparse, high-uncertainty data – particularly during high flows when field measurements become challenging and temporally limited (Mir et al., 2024; Tabesh et al., 2024; Emmett, 1980; Hubbell, 1964). In recent years, hydroacoustic methods have become increasingly important for hydrodynamics and sediment transport monitoring. Acoustic Doppler Current Profilers (ADCPs), originally developed for flow measurements, now also enable non-intrusive, continuous observation of sediment-related processes (Gartner, 2004; Kostaschuk et al., 2005). Through the emission of acoustic pulses and analysis of Doppler-shifted backscatter signals, ADCPs generate high-resolution velocity profiles (Simpson, 2001). Additionally, their bottom-tracking capability measures motion relative to the riverbed, offering valuable insight into bed dynamics (Rennie and Rainville, 2006). These features allow ADCPs to function as dual-purpose instruments, providing real-time measurements of both hydrodynamic behavior and sediment transport processes, including insight into bedload and suspended load dynamics. As such, they have become indispensable tools in hydraulic engineering investigations, both in controlled laboratory settings and complex natural environments.

A substantial body of research has established that ADCPs, through their bottom-tracking functionality, can detect the apparent movement of the riverbed – a phenomenon directly correlated with active bedload transport. Foundational studies by Rennie et al., (2002) and Rennie and Villard (2004) demonstrated that bottom-track velocity (BT_Vel) can serve as a reliable proxy for bedload flux in rivers, a conclusion later reinforced by Gaeuman and Jacobson, (2006) in large sand-bed rivers. Controlled flume studies by Ramooz and Rennie (2010) have shown a strong statistical agreement (R^2 up to 0.93) between ADCP-derived velocities and physically measured bedload rates, particularly under well-defined sediment and flow conditions. In large-scale riverine environments, Latosinski et al., (2017) and Le Guern et al., (2021) confirmed the feasibility of using ADCP-DGPS (Acoustic Doppler Current Profiler integrated with Differential GPS) systems to estimate bedload transport, reporting deviations within 15–30% of traditional dune-tracking methods when proper calibration was applied. These advances underscore the ADCP's robustness as a non-intrusive surrogate for bedload assessment, provided site-specific tuning is conducted to account for factors such as frequency, grain size, bedform dynamics, and flow depth (Gaeuman and Jacobson, 2006; Conevski et al., 2021; Conevski et al., 2023). In parallel, ADCP acoustic backscatter intensity – a measure of returned signal strength – has been extensively used as an indirect indicator of suspended sediment concentration (SSC). Guerrero et al., (2016) demonstrated that backscatter data, once empirically calibrated, correlate well with measured SSC in large rivers such as the Paraná River (Argentina) and the Danube River (Hungary). Recent



65 developments have begun integrating these two modalities: bottom-track velocity and backscatter intensity, allowing multi-dimensional characterization of sediment transport regimes. For instance, Conevski et al., (2023) showed that combining bed movement velocity with riverbed backscatter improved bedload estimation across varying sediment and flow conditions.

70 Despite these innovations, significant challenges remain. The relationship between acoustic signals and sediment concentration is complex – affected by particle size, composition, and sound attenuation – requiring site-specific calibration (Thorne et al., 1991; Guerrero et al., 2016; Latosinski et al., 2017). Similarly, inferring bedload from bottom-track velocities is complicated by spatially variable bed mobility and sensor limitations. While flume studies confirm that apparent bedload velocities correlate with transport under controlled conditions, field settings introduce hydraulic and sediment heterogeneity (Conevski et al., 2020; Conevski et al., 2023). Thus, although ADCP reduces dependence on empirical rating curves, 75 reliability improves when multiple signals are fused using advanced analytics to capture nonlinear sediment-flow dynamics.

Machine learning (ML) and deep learning (DL) have emerged as powerful approaches to tackle such complex, multivariate ^L ^D ^L problems in hydrology and geomorphology (Gacu et al., 2025). In particular, data-driven models can learn the relationship between observable signals (e.g. flow velocity, turbulence, acoustic intensity) and sediment responses, without requiring explicit physical assumptions (Lund et al., 2022; Allawi et al., 2023). This is especially useful given the nonlinear and hysteric nature of sediment transport, where sediment concentration for a given flow can differ between a rising and falling hydrograph (Jing et al., 2025; Achite et al., 2025). By training on historical or experimental data, ML algorithms can capture these details. Recent studies have applied data-driven models to sediment transport prediction with impressive success. For example, Lund et al., (2022) developed boosted decision-tree models (XGBoost) to predict suspended sediment and bedload 80 across Minnesota rivers, US; the models explained approximately 70% of the variance in sediment datasets. Likewise, DL ^x models such as Long Short-Term Memory (LSTM) networks and Convolutional Neural Networks (CNNs) have demonstrated superior performance in forecasting suspended sediment concentrations (SSC) by capturing temporal dynamics and spatial patterns beyond the reach of simpler methods (Pham Van et al., 2023; Chen et al., 2022). Allawi et al., (2023) demonstrated that an LSTM model can achieve correlations of ~0.97 for daily suspended sediment load prediction in a 90 tropical river, outperforming linear regression and other ML models. Similarly, Achite et al., (2025) found that a DL network consistently surpassed traditional rating curves and other ML/DL approaches, with NSE values near 0.99 in an Algerian catchment. These results underscore both the predictive power and the importance of interpretability and generalizability for deploying ML/DL in sediment transport applications.

95 To date, studies utilizing complete ADCP datasets for ML applications remain largely unexplored. Only recently have researchers begun to experiment with ML and DL to analyze and extract insights from ADCP output. For example, Ozsahin et al., (2025) applied a suite of ML models – including Random Forest, LightGBM, and MLP (Multilayer Perceptron) – to ADCP sensor outputs for river discharge prediction, demonstrating that ensemble models can achieve near-perfect accuracy



130 2 Methodology

2.1 Study Sites and Data Collection

2.1.1 Laboratory Flume Dataset Collection

Experiments were conducted in a 16-meter-long, 0.6-meter-wide laboratory flume at the Hydraulic Engineering and Hydromechanics Laboratory, Bochum University of Applied Sciences, Germany. The flume was operated with a fixed bed slope of 0.5%. A sand bed with a median grain diameter of $D_{50} = 0.45$ mm was prepared, filling the first 11 m of the flume.
135 To regulate flow and prevent unwanted sediment transport beyond the test section, a 4 cm high block was installed at the downstream end of the sand bed.

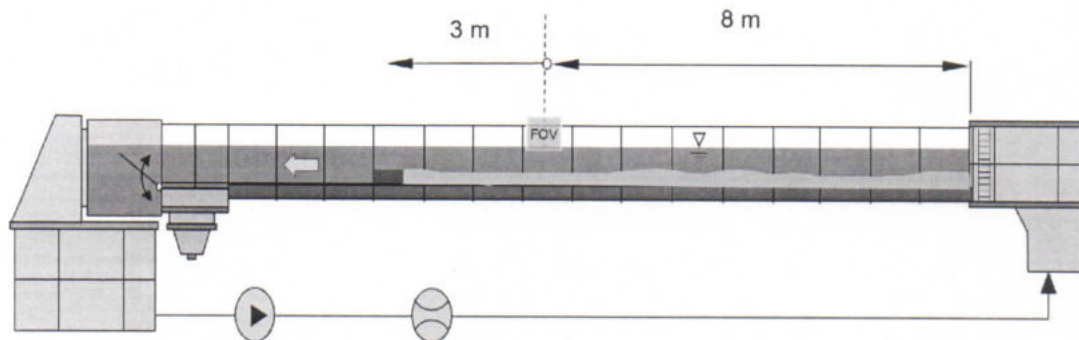


Fig. 1. Schematic of the 16 m laboratory flume showing the 11 m sand-bed section and the fixed ADCP Field of View (FOV) location.

140

The thickness of the sand bed was maintained at 3 to 4 cm throughout the experimental section. At 8 m downstream from the flume inlet, a SonTek RS5 ADCP (3 MHz broadband pulse-coherent) was installed in a stationary position, near the midpoint of the flume, to provide continuous flow profiling. The RS5 ADCP employs a four-beam Janus configuration (25° beam tilt, 3° beam width), supplemented by a vertical depth beam. The default profiling setup generates a series of closely spaced vertical cells with approximately 15% overlap, ensuring seamless spatial coverage and robust acoustic signal returns.
145 Once the flow was stabilized, data acquisition was initiated using SonTek RSQ software. The RS5 collected data at a 1 Hz sampling rate, with 30-ping ensembles used to form a single averaged measurement sample. For each run, data were logged for up to 1,620 time steps. Across fourteen different flow rates, this resulted in approximately 22,650 ensemble samples collected throughout the experimental campaign. Each ensemble sample thus corresponds to one time step - i.e., a full,
150 vertically resolved velocity profile acquired by the ADCP under steady-state flow conditions.

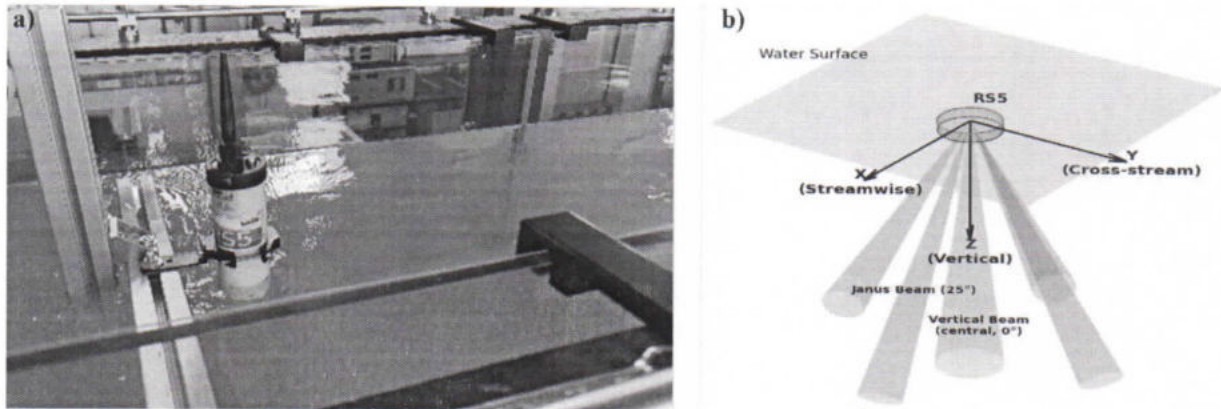


Fig. 2. Experimental setup and ADCP beam geometry. (a) RS5 acoustic Doppler current profiler (ADCP) mounted in an aluminum frame in the 16 m recirculating flume. (b) Schematic of the RS5 beam configuration showing the vertical beam (0°) and Janus beams (25°) along streamwise (X), cross-stream (Y), and vertical (Z) axes.

155

The flume discharge and flow depth were varied systematically across multiple runs to generate a range of hydraulic conditions. Under certain flows, migrating sand dunes and bedforms developed, providing varied sediment transport scenarios. The ADCP's Bottom-Track velocity readings were considered to detect bed movement during each run.

160 2.1.2 Field Dataset Collection

Field measurements were conducted on the River Stever, a mid-sized river in North Rhine-Westphalia, Germany. Data collection was performed at a fixed site across seven measurement campaigns between January 2023 and January 2024 (specifically: January 2023, June 2023, twice in August 2023, October 2023, December 2023, and January 2024). During each campaign, the survey focused on a single cross-section, where five to eight transects were performed to capture spatial variability across the section.

165

A remote-controlled rQPOD platform equipped with a SonTek RS5 ADCP was used to acquire the data. Each ensemble sample corresponds to a single vertical water velocity profile, and measurements were collected under a range of flow and seasonal conditions to represent the river's hydrodynamic variability throughout the year. In total, 5,900 ensemble samples were obtained from these campaigns. Compared to the laboratory data, the field dataset is characterized by higher uncertainty and greater heterogeneity and noise – attributable to factors such as uneven bathymetry, variable bed conditions, and instrument noise from the moving platform. Additionally, field measurements are temporally sparse, as data were acquired during discrete surveys rather than continuous monitoring.

170

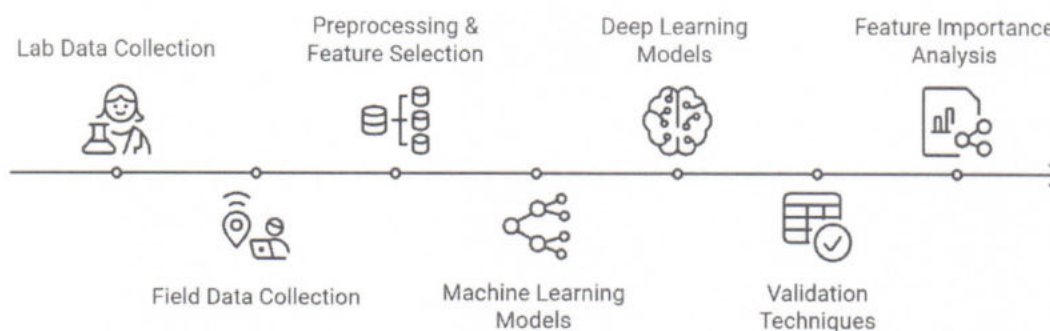


Fig. 4. Schematic workflow for Bottom-Track Velocity (BT_Vel) prediction.

2.3 Machine Learning Models

To evaluate the predictive capability of ADCP-derived features for sediment transport proxy estimation, several ensemble-based machine learning (ML) models were applied. These models were chosen for their proven performance in capturing nonlinear relationships and robustness under variable data conditions. All models were trained and evaluated using both a traditional train–test split (80/20) and 5-fold stratified cross-validation to assess generalization. Hyperparameters were unified across both laboratory and field experiments to ensure consistent comparative analysis, with parameters such as the number of estimators ($n = 100$) and learning rate (0.1, where applicable) selected based on domain knowledge and empirical validation. Features were standardized with StandardScaler fitted on the training portion only (and within each fold for cross-validation) to prevent data leakage. For regression stratification, the continuous target was discretized into 10 quantile-based bins. Performance was summarized using R^2 , MSE, and MAE (Mean Absolute Error). To maintain a like-for-like comparison with the DL baselines, we report results from fixed baseline hyperparameters (no per-model tuning for ranking). Group-blocked validation (run-blocked in the laboratory, campaign-blocked in the field) was conceptually considered but not applied in the main benchmarking due to the small number of runs/campaigns; its implications are discussed in Section 4.5 (Limitations).

2.3.1 Ensemble Tree-Based Models

The study utilized five ensemble tree-based algorithms that highlight both bagging and boosting approaches. Random Forest is a bagging-based ensemble method that constructs multiple decision trees using bootstrapped datasets and random feature selection. It is known for its robustness to overfitting, ability to handle noisy or high-dimensional data, and strong performance across a range of regression tasks (Cutler et al., 2007). Gradient Boosting builds decision trees sequentially by minimizing prediction errors through gradient descent. It emphasizes residual fitting and is effective in capturing complex feature interactions, though it may be sensitive to noise and requires careful regularization (Friedman, 2001). Extreme



245 Gradient Boosting (XGBoost) enhances gradient boosting by incorporating L1/L2 regularization, column subsampling, and parallelization. Its computational efficiency and scalability make it a preferred choice for structured regression tasks in environmental and hydrological domains (Chen and Guestrin, 2016). LightGBM is a leaf-wise gradient boosting algorithm based on histogram binning that improves computational speed and memory efficiency, and its ability to handle large datasets and support categorical features make it well suited for environmental prediction applications (Ke et al., 2017). CatBoost is a boosting framework designed to handle categorical variables natively and mitigate prediction shift via ordered 250 boosting. It is particularly advantageous when feature importance and generalization are prioritized under noisy conditions (Prokhorenkova et al., 2018). Together, these algorithms provide a comprehensive ensemble framework balancing accuracy, interpretability, and robustness across both laboratory and field datasets.

2.3.2 Stacking Ensemble

Stacking Regressor was employed to enhance generalization and integrate the complementary strengths of individual 255 learners. The two-level ensemble architecture consisted of a base layer combining Random Forest and Gradient Boosting models, with a Gradient Boosting Regressor acting as the meta-learner. This architecture aims to balance bias-variance trade-offs by combining predictions from diverse model families. Such stacked approaches have shown improved robustness in hybrid modeling contexts, particularly where no single algorithm dominates across validation folds.

All models followed the preprocessing and validation protocol described above, including leak-free scaling (fit on train / per 260 fold) and identical random seeds for reproducibility. Comparative performance across the laboratory and field datasets is reported in Sections 3.1.2 and 3.2.2.

2.4 Deep Learning Models

265 Six deep learning (DL) architectures were implemented identically for the laboratory and field datasets. These included a feed-forward ANN, a 1D CNN, three recurrent models (LSTM, GRU, RNN), and a hybrid, selected to represent common DL families used for structured and sequential hydroacoustic data. To ensure like-for-like comparison with the ML baselines and across DL families, we fixed one baseline per model and used the same preprocessing, loss, and evaluation regime. Features were standardized with a StandardScaler fitted on the training portion only (and per fold in cross-validation) to avoid leakage.

2.4.1 Evaluation protocols

270 Models were assessed under two regimes: an 80/20 hold-out split and 5-fold stratified cross-validation (CV) with 10 quantile bins on the continuous target. For the hold-out split, we swept batch size over {6, 8, 10, 12, 16, 20, 24, 32, 40, 64} using train-only validation; the batch size with the lowest validation loss was selected, after which the model was retrained on the training set with early stopping (patience 5–7; best weights restored) and evaluated once on the untouched test set. For CV, scaling was performed per fold, with batch_size = 32, ≈30 epochs, and the same early-stopping criterion. Evaluation metrics



variability (true temporal changes in river hydraulics) and epistemic uncertainty (limited campaign count and missing covariates). Second, suspended sediment concentration (SSC) and bedload transport were not directly measured; instead, Bottom-Track Velocity (BT_Vel) was used as a proxy, which introduces representational uncertainty. Third, potential sensor-specific biases and variations in deployment geometry (e.g., changes in Bin Distance) were not corrected through independent calibration. Fourth, DL models were trained on relatively small datasets, constraining their generalization capacity. Fifth, external hydro-meteorological drivers such as rainfall, upstream sediment supply, and antecedent flow history were excluded, despite their influence on sediment transport. In addition, exploratory refinements (e.g., a deeper ANN and an optimized LSTM) improved their absolute performance and ranking relative to the baselines, as expected. However, to maintain fairness and a like-for-like comparison across the full set of ML/DL models, only standardized baseline configurations are reported. Similarly, Bayesian hyperparameter searches produced marginal gains without changing the broader performance patterns and were therefore excluded from the reported benchmarking.

4.6 Future Outlook

Future work should aim to expand the dataset, both temporally and spatially, through increased field campaigns and incorporation of more diverse hydraulic conditions. Direct measurements of SSC and bedload transport would enhance model calibration and validation. Hybrid modeling approaches that integrate physical modeling (e.g., Delft3D or CFD) with data-driven methods may improve both accuracy and interpretability. Real-time deployment of ADCPs combined with ML or data assimilation may support more continuous monitoring of sediment transport dynamics, though practical implementation will require addressing data volume, noise, and model updating. Furthermore, future efforts could explore robust data augmentation techniques, domain adaptation, and multi-target modeling to enhance the applicability of these models across different riverine systems.

Overall, this study demonstrates the potential of ADCP-derived features in proxy modeling of sediment dynamics, while highlighting the importance of validation strategy, model selection, and environmental context. For real-world applications, efforts should prioritize increasing training data volume, applying regularization or data augmentation for DL models, and exploring hybrid modeling frameworks that balance robustness and expressiveness. These strategies are likely to be important for enabling data-driven sediment transport tools at operational scales in morphodynamically active riverine systems and furthering the integration of hydroacoustic sensing with modern predictive analytics.

Conclusions

This study provided a systematic evaluation of Acoustic Doppler Current Profiler (ADCP)–derived features as proxies for sediment transport dynamics in both controlled flume experiments and natural riverine conditions. Using Bottom-Track



- 665 Gartner, J. W.: Estimating suspended solids concentrations from backscatter intensity measured by acoustic Doppler current profiler in San Francisco Bay, California, *Mar. Geol.*, 211, 169–187, <https://doi.org/10.1016/j.margeo.2004.07.001>, 2004.
- Guerrero, M., Rüther, N., Szupiany, R., Haun, S., Baranya, S., and Latosinski, F.: The acoustic properties of suspended sediment in large rivers: Consequences on ADCP methods applicability, *Water*, 8, 13, <https://doi.org/10.3390/w8010013>, 2016.
- 670 Hubbell, D. W.: Apparatus and techniques for measuring bedload, U.S. Geological Survey, Washington, D.C., U.S. Geological Survey Water-Supply Paper, 1748, 74 pp., 1964.
- Jing, T., Zeng, Y., Fang, N., Dai, W., and Shi, Z.: A review of suspended sediment hysteresis, *Water Resour. Res.*, 61, e2024WR037216, <https://doi.org/10.1029/2024WR037216>, 2025.
- Kakarla, S. M., Abuomar, O., Abojaradeh, M., Shaqadan, A., Alshoulat, I., and Omari, A.: Acoustic Doppler current profiler data analytics using a hybrid of machine learning methods, in: 2nd International Engineering Conference on Electrical, Energy, and Artificial Intelligence (EICEEAI), IEEE, Zarqa, Jordan, 2023. ✖
- 675 Ke, G., Meng, Q., Finley, T., Wang, T., Chen, W., Ma, W., Ye, Q., and Liu, T.-Y.: LightGBM: A highly efficient gradient boosting decision tree, in: *Advances in Neural Information Processing Systems 30 (NeurIPS 2017)*, Long Beach, USA, 4–9 December 2017, Curran Associates, Inc., Red Hook, NY, USA, 3149–3157, 2017.
- Kostaschuk, R., Best, J., Villard, P., Peakall, J., and Franklin, M.: Measuring flow velocity and sediment transport with an acoustic Doppler current profiler, *Geomorphology*, 68, 25–37, <https://doi.org/10.1016/j.geomorph.2004.07.012>, 2005.
- 680 Latosinski, F. G., Szupiany, R. N., Guerrero, M., Amsler, M. L., and Vionnet, C.: The ADCP's bottom track capability for bedload prediction: Evidence on method reliability from sandy river applications, *Flow Meas. Instrum.*, 54, 124–135, <https://doi.org/10.1016/j.flowmeasinst.2017.01.005>, 2017.
- Le Guern, J., Rodrigues, S., Geay, T., Zanker, S., Hauet, A., Tassi, P., Claude, N., Jugé, P., Duperray, A., and Vervynck, L.: Relevance of acoustic methods to quantify bedload transport and bedform dynamics in a large sandy-gravel-bed river, *Earth Surf. Dynam.*, 9, 423–444, <https://doi.org/10.5194/esurf-9-423-2021>, 2021.
- 685 Lund, J. W., Groten, J. T., Karwan, D. L., and Babcock, C.: Using machine learning to improve predictions and provide insight into fluvial sediment transport, *Hydrol. Process.*, 36, e14648, <https://doi.org/10.1002/hyp.14648>, 2022.
- Mir, A. A., Patel, M., Albalawi, F., Bajaj, M., and Tuka, M. B.: A comparative ensemble approach to bedload prediction using metaheuristic machine learning, *Sci. Rep.*, 14, 25725, <https://doi.org/10.1038/s41598-024-75118-5>, 2024.
- 690 Ozsahin, D. U., Emegano, D. I., Uzun, B., and Ozsahin, I.: Machine learning approaches for river discharge prediction using acoustic Doppler current profiler (ADCP) data, in: *Climate change and water resources in Mediterranean countries*, Gökçekuş, H., Kassem, Y. (Eds.), Springer Nature Switzerland, Cham, 175–188, 2025.
- Pham Van, C., Le, H., and van Chin: Estimation of daily suspended sediment concentration in the Ca River Basin using a sediment rating curve, multiple regression, and long short-term memory model, *J. Water Clim. Change*, 14, 4356–4375, <https://doi.org/10.2166/wcc.2023.229>, 2023.